ELSEVIER

Physica E 8 (2000) 154–163

PHYSICA E

www.elsevier.nl/locate/physe

Engineering quantum-dot lasers

J.H. Marsh *, D. Bhattacharyya, A. Saher Helmy, E.A. Avrutin, A.C. Bryce

Department of Electronics and Electrical Engineering, University of Glasgow, Glasgow G12 8QQ, Scotland, UK

Abstract

We discuss recent progress in the engineering of quantum-dot (QD) lasers, focusing on the spectral output, dynamics and techniques for integration. Two approaches to such engineering are discussed. Firstly, it is suggested that control of lasing spectra in QD lasers is possible by making use of waveguiding-related phenomena (substrate leakage and reflection) which, in unoptimised laser structures, result in the mode grouping effect (quasiperiodic spectral modulation). Secondly, first experimental studies of quantum dot intermixing are reported, suggesting that this technique is capable of both improving the performance of active QD media and integrating active QD sections with passive waveguides. © 2000 Elsevier Science B.V. All rights reserved.

PACS: 42.55; Px: 68.35; ct: 71.24.+q: 73.20; Dx: 85.30.V

Keywords: III–V semiconductors; Semiconductor lasers; Quantum dots; Interface diffusion

1. Introduction

The predicted advantages of quantum dot (QD) lasers include low-temperature sensitivity of the threshold current, high modulation frequency and low chirp [1–3]. Self-organized growth, using the Stranski–Krastanow mechanism, is considered to be the most promising technique for in situ fabrication of quantum dot arrays as a semiconductor laser gain medium [4–6]. Unfortunately, the low confinement energies, inhomogeneous broadening due to dot size fluctuations, and factors such as carrier transport delays have so far limited the performance of QD lasers, especially at room temperature [7,8]. The introduction of vertically coupled QD layers has improved the lasing performance at room temperature by increasing the modal gain thus overcoming the gain saturation effect [9,10]. Recently, substantial reductions in the threshold-current densities of quantum-dot (QD) lasers have been achieved [3,11], setting the scene for utilising devices containing QD structures [11,12]. However, other problems, such as those related to spectral and dynamic performance, still need to be addressed. Here we discuss recent progress in the engineering of QD lasers, focusing on the spectral output, dynamics and techniques for integration. The paper is organised as follows. Section 2 deals with specific effects in quantum-dot lasers related to waveguide properties and suggests ways they can be used to engineer the spectral and dynamic

* Corresponding author. Tel.: +44-141-3304790; fax: +44-141-3306002.

E-mail address: j.marsh@elec.gla.ac.uk (J.H. Marsh).

1386-9477/00/$ - see front matter © 2000 Elsevier Science B.V. All rights reserved.
PII: S1386-9477(00)00133-8

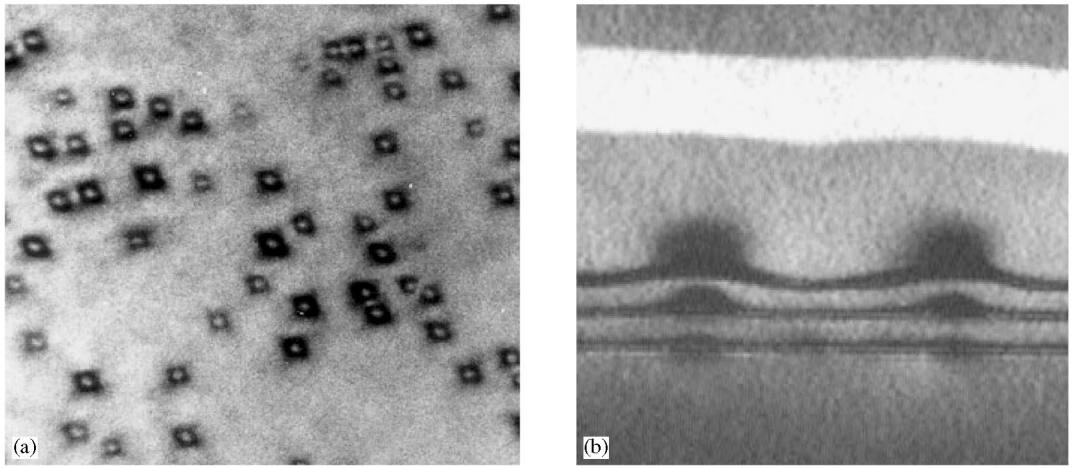

Fig. 1. Plan view (left) and cross-sectional (right) TEM images of vertically stacked InAs/GaAs quantum-dot structure with 4 nm separation layer thickness.

behaviour of the lasers and to characterise the physical processes in the lasers. Section 3 discusses the technique of quantum dot intermixing and its potential for monolithic integration of QD lasers as well as for engineering laser performance. Section 4 summarises the results and presents general conclusions.

2. Engineering QD laser spectra by adjusting waveguide parameters

2.1. Lasing spectra: Experimental

The structures used in our work were grown by MOCVD and contained three- and five-fold stacked self-organised InAs/InGaAs QD layers [13]; for details of the structures, see Table 1. Plan-view and cross-sectional transmission electron microscope images of three-fold QD samples are shown in Fig. 1. The image in Fig. 1(a) shows a dot density around 4×10^{10} cm^{-2} with dots having a lateral size of 15–18 nm. The apparent dot bases are close to being square-shaped, with one side of the bases approximately oriented along $\langle 1\,0\,0 \rangle$. The dots, however, appear in the TEM image to be slightly elongated along one of the $\langle 1\,1\,0 \rangle$ directions. The lasers, fabricated from five-fold structures grown under identical conditions, were defined using photolithography, dry etched to form ridge structures 4 μm wide and 1.45 μm high, and cleaved to lengths between 500 μm and 1.5 mm.

Table 1
QD laser structure used in spectral and dynamic studies

Contact layer	p^+ GaAs	0.6 μm
Upper cladding	p-$Al_{0.5}Ga_{0.5}As$	1.0 μm
Superlattice	GaAs/$Al_{0.5}Ga_{0.5}As$	20 × (2, 2 nm)
Inner cladding	GaAs	70 nm
3–5 ×	InAs QDs	1.22 ML
Stacked QDs	Cap layer GaAs	4 nm
Inner cladding	GaAs	70 nm
Superlattice	GaAs/$Al_{0.5}Ga_{0.5}As$	20 × (2, 2 nm)
Lower cladding	n-$Al_{0.5}Ga_{0.5}As$	1.0 μm
Buffer	n-GaAs	0.5 μm
Substrate	n-GaAs (1 0 0)	

Figs. 2–3 show the spectral characteristics of the 1.0 and 1.35 mm long laser samples, respectively. Lasing emission from the 1.0 mm long devices is at $\lambda = 1077$ nm, and lies on the high-energy side of the PL peak (1155 nm at room temperature), indicating that excited dot states may be contributing to the room temperature lasing process. The spectra contain several groups of longitudinal modes which are separated by approximately 2 nm (i.e. about 10 intermodal intervals) and are excited one by one with increasing bias current (in Fig. 2, the groups are seen as broadened "modes" due to the limited resolution of the spectrum analyser). Other workers

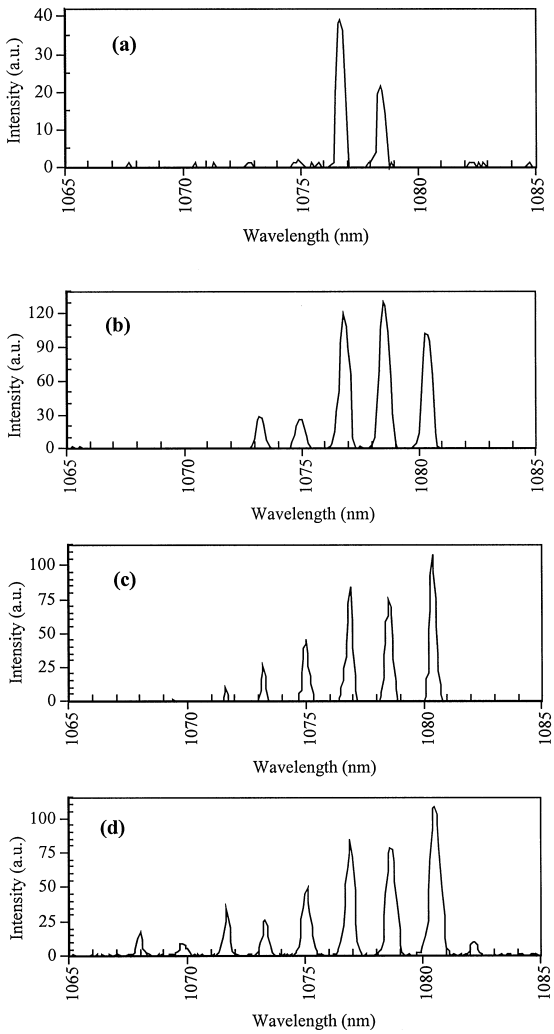

Fig. 2. Pulsed spectra of 1.0 mm long and 4 μm wide QD ridge waveguide lasers with increasing bias current at room temperature: $I/I_{th} = 1.04$(a), 1.24(b), 1.44(c), 1.65(d).

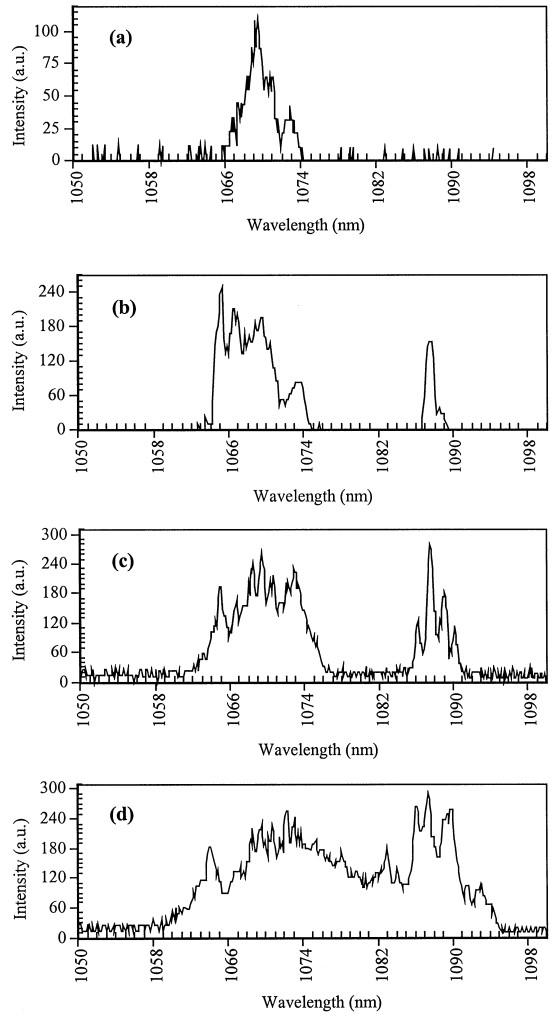

Fig. 3. Pulsed spectra of 1.35 mm long and 4 μm wide QD ridge waveguide laser with increasing bias current at room temperature: $I/I_{th} = 1.04$(a), 1.24(b), 1.44(c), 1.65(d).

have reported similar behaviour [14,15]. The spectra observed from the longer lasers are significantly different. Again lasing is shifted slightly towards shorter wavelengths from the PL maximum (1088 nm in this case) but, in addition, a broader structure is centred at an even shorter wavelength (about 1068 nm). This second peak has been also observed by other authors [16] and tentatively attributed either to transitions from the excited states or to emission by two groups of dots with different average sizes. An additional modulation with a period ($\sim$ 1.5–2 nm) is present in both envelope peaks, similar to, but less pronounced than, that seen from the 1 mm long sample.

2.2. *Lasing spectra: theoretical considerations*

We believe the most probable origin of the mode grouping effect lies in the waveguide peculiarities of the GaAs/InGaAs lasers. The effect was first reported for quantum-well lasers [17] and may be explained as

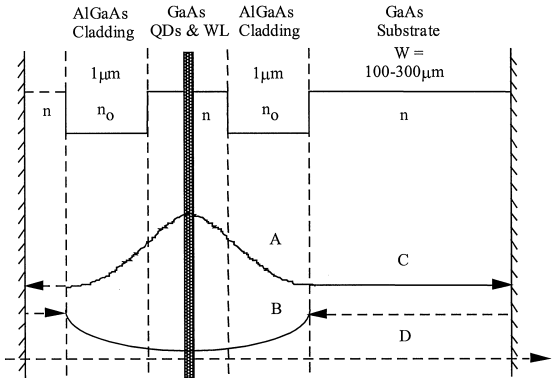

Fig. 4. Illustration of mode selectivity by substrate leakage and reflection in a laser waveguide.

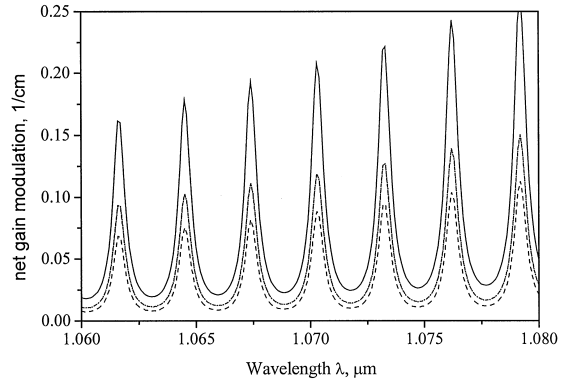

Fig. 5. Calculated contributions of leakage loss and confinement factor modulation to total net gain modulation in a quantum-dot laser. Top line (solid): total net gain modulation; bottom line (dashed): leakage loss contribution; middle line (dashed–dotted): confinement modulation.

follows [13,18]. The waveguide transverse mode decays exponentially in the semi-infinite cladding layers of the laser waveguide (Fig. 4). The typical thickness of a cladding layer in a semiconductor laser, (d_c) is $\sim$ 1–2 μm, ($d_c = 1$ μm in our structure) and is sufficiently wide to form a good waveguide mode, almost identical to that of an ideal waveguide. Nevertheless, the waveguide mode has a finite magnitude, $\exp(-pd_c)$ at the edge of the cladding layer, where p is the inverse decay length ($p \sim 5$ μm^{-1} in the laser structure studied here). A small fraction of the mode will then leak out of the cladding, propagating as $C\exp(iqx)$ through the transparent substrate of thickness h_s (Fig. 4). Part of this leaking mode is reflected back from the bottom of the substrate, returning towards the cladding with an amplitude $D\exp(-iqx)$, where $|D| = r|C|$, r being an effective reflection coefficient assigned to the substrate bottom [17]. The net loss, $\Delta\alpha_s$, associated with leakage into the substrate is then proportional to $|C|^2 - |D|^2$. By assuming continuity of the mode profile and its derivative, Arzhanov et al. [17] showed that

$$\Delta\alpha_s(\lambda) = \Delta\alpha_o \frac{\exp(-2pd_c)(1-r^2)}{1+r^2-2r\cos(\psi-\varphi(\lambda))}, \qquad (1)$$

where $\varphi(\lambda) = 2qh_s + \varphi_0$, $\exp(i\psi) = (p+iq)/(p-iq)$, and φ_0 is the effective phase shift due to reflection from the substrate bottom. The prefactor, $\Delta\alpha_0$, is of order $1/d_{eff}, d_{eff}$ being the effective transverse size of the mode. As d_{eff} is typically ~ 1 μm in a GaAs/AlGaAs laser, this gives $\Delta\alpha_0 \sim 10^4$ cm^{-1}.

We see from Eq. (1) that the leakage-related loss is modulated as the substrate path length, $\varphi(\lambda)$, changes. This results in a modulation in the net modal gain $g_m(\lambda) \approx \Gamma g - \Delta\alpha_s - \alpha_o$, where Γ is the optical confinement factor, g is the material gain and α_o denotes other losses in the cavity. In addition to the wavelength-dependent *loss* term, the substrate leakage and interference result [13,18] in a modulation $\Delta\Gamma = \Gamma - \Gamma_0$ of the optical confinement, Γ_0 being the value calculated without leakage. Our numerical simulations show that the resulting modal gain modulation $\Delta\Gamma g$ (g being the material gain at threshold) is approximately proportional, and of comparable magnitude, to $\Delta\alpha$ for a typical structure of the type discussed above (Fig. 4). The total modal gain modulation is $\Delta g_m(\lambda) \approx \Delta\Gamma g - \Delta\alpha_s$; the amplitude values are of the order of 0.1 cm^{-1} (Fig. 5) and thus constitute about 1% of the total cavity loss (about 20 cm^{-1} for the laser structure studied here). As regards the modal gain modulation period $\Delta\lambda$, it easily follows from Eqs. (1) that it is inversely proportional to the substrate thickness h_s: $\Delta\lambda = \pi\lambda/qh_s$. With the material and waveguide parameters used in this work, a modulation period of 2–4 nm corresponds to a substrate 150–300 μm thick, in agreement with what is commonly obtained by substrate thinning.

Although modal gain modulation due to substrate leakage has been observed in InGaAs/AlGaAs

quantum well lasers, the mode grouping in these lasers is not very pronounced; instead, nearly single-mode spectra with some mode hopping have been observed [17]. However, we can expect the effect to be more marked in InGaAs/AlGaAs quantum-dot lasers where the lasing spectra are much broader than those typical in CW operated QW lasers – with or without mode grouping. We believe the reason behind this is a combination of a broad gain spectrum, which is due to the strong inhomogeneous broadening arising from QD size dispersion, and an increase in gain nonlinearities in quantum dots compared to bulk or quantum well media. To investigate this in some more detail, we have compared the experimentally observed spectra with those obtained from a multimode rate-equation model [13]. The model includes the standard rate equations for carrier (populated dot) density N and intensity of modes S_m (m being the mode number).

$$\frac{\mathrm{d}N}{\mathrm{d}t} = P - \frac{N}{\tau} - \sum_m g_m S_m, \tag{2a}$$

$$\frac{\mathrm{d}S_m}{\mathrm{d}t} = \beta\frac{N}{\tau} + \left(\Gamma g_m - \frac{1}{\tau_{\mathrm{ph}}^{(m)}}\right) S_m, \tag{2b}$$

where most of the symbols have their standard meaning, with P standing for the pumping term (capture minus escape) and the modal photon lifetimes $\tau_{\mathrm{ph}}^{(m)} = 1/v_{\mathrm{g}}\alpha_m$ include the total loss (net gain) modulation as discussed above. For the modal gain g_m we use the well-known simple approximation

$$g_m = A(N - N_{\mathrm{t}})(1 - b^2m^2)\left(1 - \sum_k \varepsilon_{mk} S_k\right), \tag{3}$$

where A and N_{t} are the gain cross-section and the transparency carrier density, the parameter $b \ll 1$ is a measure of the width of the gain spectrum, and the coefficients ε_{mk} phenomenologically introduce mode coupling due to the fast gain nonlinearities. In principle, at least two groups of effects may be expected to contribute to these nonlinearities. The first effect is short-scale spatial hole burning, caused by depletion of population inversion at the antinodes of the standing wave(s) corresponding to the longitudinal mode(s) lasing initially. The second group of effects is related to spectral hole burning, caused by depletion of population inversion in those dots whose electron–hole level separation is resonant with the lasing mode energy, and related population pulsations (pulsation-induced four-wave mixing is neglected because mode grouping makes longitudinal modes significantly non-equidistant).

It is already known that, for bulk and QW active media, effects associated with both spectral [19] and spatial [20] hole burning are reasonably well described by an approximate scaling equation of the form

$$\varepsilon_{mk} \approx CA\tau_\varepsilon \frac{1 + \alpha\Delta\tau_\varepsilon(m-k)}{1 + [\Delta\tau_\varepsilon(m-k)]^2}. \tag{4}$$

Here C is a dimensionless coefficient that depends on the type of the nonlinearity and the cavity geometry; $\Delta = v_{\mathrm{g}}/2L$ is the angular frequency separation between longitudinal modes (v_{g} being the group velocity of light); $\alpha - 1$ is a numerical parameter related, though not necessarily equal, to the Henry line-width enhancement factor ($\alpha > 0$ for the case of spectral nonlinearities [19]; $\alpha < 0$ for spatial effects, [20]). Finally, τ_ε in Eq. (4) is the nonlinearity relaxation time, i.e. the relaxation time through carrier transport effects of the self-induced grating in the case of the spatial effects, or the carrier relaxation time in the case of spectral effects.

In the simulations, the parameters $(C, \alpha, \tau_\varepsilon)$ related to gain nonlinearities were treated as adjustable parameters. The simulations show that, in the absence of the quasi-periodic net gain modulation, the effect of nonlinearities is to cause the lasing spectrum to broaden smoothly with increasing pump current. In the presence of the net gain modulation, the broadening takes the form of an increase in the number of mode groups involved in lasing (Fig. 6). As seen in Fig. 6, we are able to simulate a spectrum similar to that seen experimentally, the only discrepancy being a slightly overestimated red shift of the laser spectrum with current. In the simulation, we assigned the gain nonlinearity a value of $\varepsilon_{\mathrm{s}} = CA\tau_\varepsilon \sim 10^{-14}$ cm^3. This is about three orders of magnitude larger than the values (10^{-18}–10^{-17} cm^3) typically encountered in bulk and quantum well materials. Most of this increase may be associated, in the light of Eq. (4), with the increased oscillator strength of the optical transitions, represented by the gain constant A, in QD active media ($A \sim v_{\mathrm{g}} \times 10^{-13}$ cm^2, as opposed to $A \sim v_{\mathrm{g}}(10^{-16}$–$10^{-15})$ cm^2 in bulk and QW materials). The remaining factor, of the order of several times to one order of magnitude, we ascribe to the slower nonlinearity relaxation times in QDs.

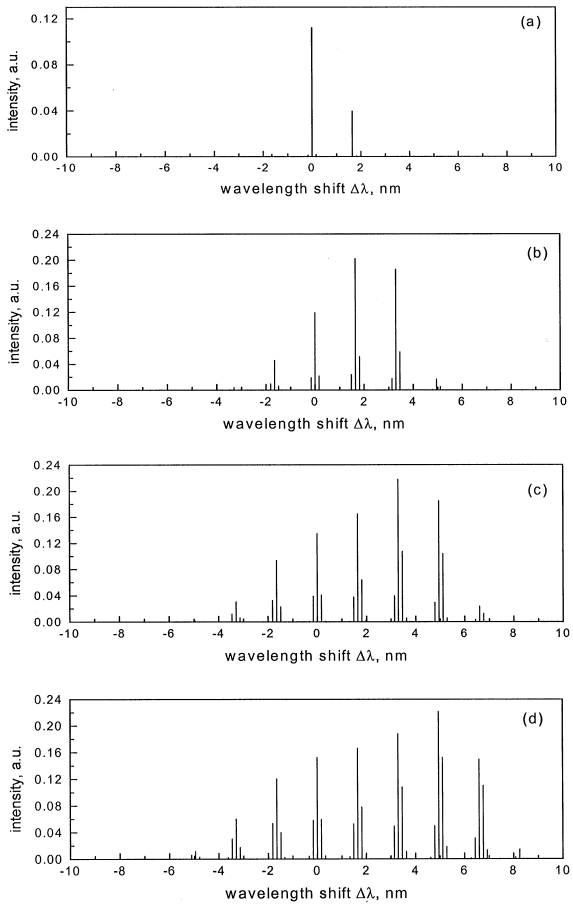

Fig. 6. Rate-equation simulation of steady-state lasing spectra in a laser with a periodic spectral modulation of the cavity loss. Pumping current $I/I_{th} = 1.05$(a), 1.25(b), 1.45(c), 1.65(d).

Localisation of carriers in dots is expected to slow down the energy relaxation of carriers, hence causing an increase in spectral hole burning and associated nonlinearities, and impede transport effects such as diffusion, hence increasing spatial hole burning [21]. However, a *positive* value of $\alpha = 0.7$ was used in Eq. (4) to reproduce the sign of the lasing spectrum asymmetry and the red spectral shift of the lasing peak. This implies that the well-developed multimode regime studied here is likely to be dominated by nonlinearities other than spatial hole burning – for example, by spectral hole burning and, possibly, population pulsations. We note, also, that the value of $\tau_\varepsilon = 150$ fs that we used to fit the experimental results was only 2–3 times greater than the typical values encountered in bulk and quantum well media. This agrees with recent four-wave mixing and pump–probe measurements on QD amplifiers where little, if any, increase in the characteristic relaxation times was observed [22,23]. In other words, effects of carrier localisation need not be particularly strong to have a significant effect on laser spectra.

It has been found [13] that structures with complex dynamic spectra such as those shown in Fig. 3 also display complex dynamic behaviour at turn-on, with very strong relaxation oscillation damping and satellite peaks in the relaxation oscillation train. This latter feature can be explained [13] by postulating slow carrier exchange between different groups of lasing dots separated in space and/or energy. This slow carrier exchange may be due to the same carrier localisation effects that slow down carrier relaxation and lead to strong nonlinearities and result ultimately in the pronounced mode grouping.

2.3. Implications for engineering lasing spectra

The experimental and theoretical results above form a consistent picture of the mode grouping effect, thus giving us the confidence to make some design recommendations. For many laser applications, e.g. for mode-locked operation, the mode grouping effect is detrimental and needs to be eliminated. Our analysis suggests that this can be achieved by careful optimisation of the waveguide structure, mainly by ensuring that the cladding layers are sufficiently thick. For example, experimentally we observed no mode grouping in lasers with cladding layers 1.8 μm thick. Alternatively, control of waveguide selectivity in a QD laser could be put to practical use, firstly as an investigative tool, e.g. to quantify the effects of spectral and spatial hole burning in quantum dot lasers and extract relevant parameters, along the lines outlined above. A further step would be to use the leakage and reflection effects to engineer the lasing spectra. In a radical design, one could opt for a waveguide structure with a thin cladding, thin substrate and smooth lower surface (high reflectance, r) to suppress lasing from all but one group of a few longitudinal modes, or even one single mode. This would eliminate undesired features related to broad lasing spectra, but at the expense of a further

Table 2
QD structure used in intermixing studies

Contact	p^+ GaAs	0.6 μm
Graded	p-$Al_{0.3\rightarrow 0}$	0.1 μm
Upper cladding	p-$Al_{0.3}Ga_{0.7}As$	1.2 μm
Barrier	GaAs	95 nm
Single layer QDs	$In_{0.5}Ga_{0.5}As$	4 ML
Barrier	GaAs	95 nm
Lower cladding	n-$Al_{0.3}Ga_{0.7}As$	1.2 μm
Graded layer	n-$Al_{0\rightarrow 0.3}$	0.1 μm
Buffer	n-GaAs	0.3 μm
Substrate	n-GaAs (1 0 0)	

decrease in the external quantum efficiency. The most satisfactory way to narrow QD laser spectra is, of course, to grow a laser structure with a uniform and narrow dot size distribution. This is arguably the greatest challenge presently facing QD laser technology; some of the possibilities of improving the homogeneity of the size distribution are discussed in the next section.

3. Quantum-dot intermixing for engineering QD laser properties

The previous section concentrated on tailoring the properties of the quantum dot laser waveguide to engineer the laser properties; here we concentrate on trimming the properties of the active layer. Quantum-dot intermixing appears to be a very promising way to achieve this goal.

Initial work on the thermal treatment of QDs was undertaken recently to investigate the possibilities of subsequent growth of high-quality GaAs and AlGaAs layers [24,25]. This work revealed that the 3D confinement of QDs could be preserved after annealing, hence suggesting that annealing can be used to give post-growth control of the band gap of QD structures. However, control of the band gap of laser diode structures must be selective for useful integration, allowing the integration of active and passive devices on the same chip. Techniques originally developed for quantum-well intermixing are investigated in this section as means of QD intermixing (QDI) [26].

The structure used in this work was a p–i–n separate confinement heterostructure grown using

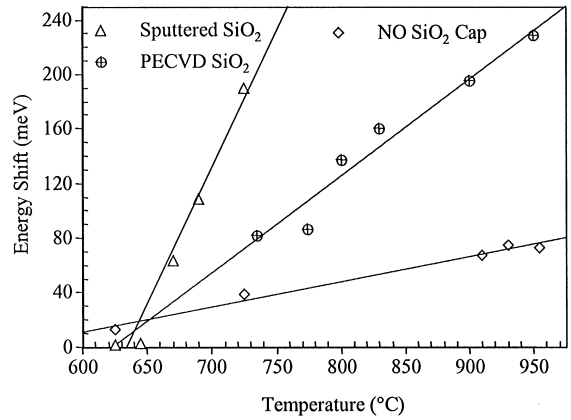

Fig. 7. QD band-gap shift as a function of annealing temperature for the different samples.

MBE and containing a single layer of self-organised $In_{0.5}As_{0.5}As$/GaAs QDs as shown in Table 2. Two intermixing techniques were investigated: impurity-free vacancy disordering (IFVD) using PECVD SiO_2 [26], and irradiation-damage-induced intermixing using sputtered SiO_2 [27]. Samples annealed without any caps were also used as controls. All samples were annealed *epi*-layer down on a fresh piece of GaAs at different temperatures for 60 s. After etching the top contact layer and the upper cladding of the structure, PL measurements were carried out at 77 K using an Ar^+ laser ($\lambda = 514$ nm).

Samples annealed without a cap layer show blue shifts of up to 77 meV as can be seen in Fig. 7, but the PL line widths were broader than that of the as-grown sample, as can be seen in Fig. 8. Samples annealed with PECVD SiO_2 show blue shifts of up to 228 meV, with a significant *narrowing* of the PL line width, from 80 meV for as-grown samples to 27 meV when annealed at 950°C. Intermixing will modify the strain distribution, and lead to a blue shift due to alloying and a red shift due to the decreased quantum confinement. It appears that, as for strained and unstrained QW structures, the alloying effect dominates. The line-width narrowing can be explained by assuming that the intermixing increases the geometrical size of dots whilst preserving the absolute size dispersion, hence leading to a decrease in the relative dispersion and to line-width narrowing. Further experimental and

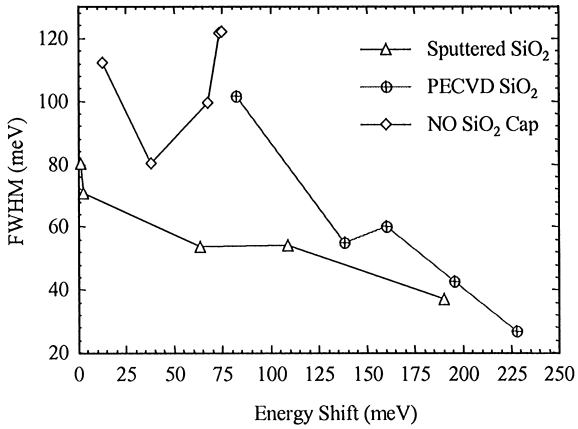

Fig. 8. QD emission line width as a function of increase in band-gap energy.

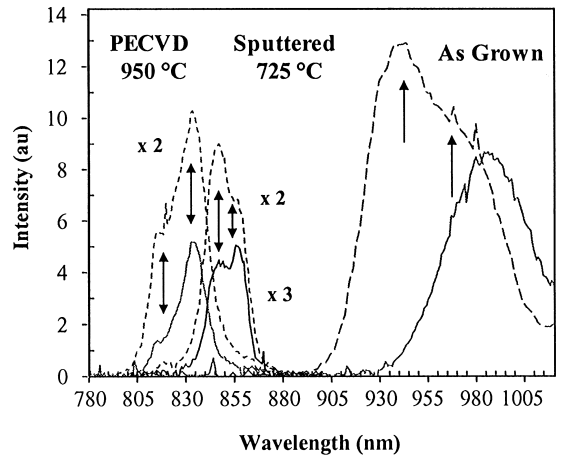

Fig. 9. PL from as-grown and intermixed samples at two excitation power densities.

theoretical studies will be necessary to verify this. The band-gap shifts and the line-width narrowing results observed using PECVD SiO_2 agree with previous reports for similar structures [25]. Similar blue shifts, of up to 190 meV in the PL peak position and a line width of 37 meV for samples annealed at 725°C, were observed for samples annealed with sputtered SiO_2. In both sets of samples, the energy shift is approximately linear over a wide range of annealing temperatures, as can be seen in Fig. 7. To ensure that the structure retains a confinement potential after intermixing, band filling of the QD excited states was investigated. PL signals were therefore acquired for two excitation power densities. As can be seen in Fig. 9, excited states were seen in both as-grown and intermixed samples, confirming that the QD confinement potential is retained after intermixing.

Annealing without dielectric caps provides the capability of obtaining differential band-gap shifts, when combined with PECVD SiO_2 with annealing at 950°C. However, processing strained structures such as self-organised QDs, in this temperature range will introduce degradation in the PL intensity, as has been reported previously [24,25]. With sputtered and PECVD SiO_2 caps, however, a differential shift can be achieved with annealing at 725°C, as can be seen in Fig. 7. The use of such a low annealing temperature will ensure good material quality for the subsequent fabrication of laser diodes. In contrast to annealing with silica caps, which enhances the group III inter-diffusion in the QD layer vicinity, annealing without dielectric caps also results in the loss of As from the sample surface, hence generating a large number of group V vacancies. Interesting effects resulted from such processing as can be seen in Fig. 8, where the line width of the samples annealed without caps increases as a function of the extent of intermixing [24,25]. This also suggests that, while Ga out-diffusion can be used to control the band gap of the QD and give line-width narrowing, As out-diffusion has a detrimental effect on the emission line width. Although further systematic studies are being carried out to explain such observations, comprehensive modelling tools for the effect of strain and compositional change on the QD energy levels are needed to analyse the results.

4. Summary

We have described two approaches to engineering the properties of QD semiconductor lasers: the first of these is through design of the waveguiding properties of the laser, and the second is to modify the active medium by quantum-dot intermixing. In the first part of the paper, we discussed the mode grouping effect in QD lasers, showing that the

origin of the effect is leakage of the transverse mode through the cladding layers followed by reflection from the substrate. This effect is purely electromagnetic and is not restricted to QD lasers, but the effect is significantly increased in QDs through the strong optical nonlinearities arising from carrier localisation. Possible uses of this effect for characterisation of laser nonlinearities and trimming lasing spectra have been suggested. In the second part of the paper, we demonstrated selective control of the luminescence from QD layers by quantum dot intermixing techniques (impurity-free vacancy disordering and irradiation-damage-induced intermixing). Substantial (~ 100 meV) differential emission peak shifts, sufficient for integrating active and passive waveguides, as well as significant spectral narrowing, have been demonstrated.

We conclude by pointing out a certain asymmetry between the two approaches to QD engineering discussed here. On the one hand, the mode grouping and associated effects are now reasonably well understood; but the potential of their use for engineering laser properties is somewhat limited as discussed in Section 2.3. The studies of quantum-dot intermixing, on the other hand, are at present at a relatively early stage, with extensive experimental and theoretical investigations needed to achieve a thorough understanding of the mechanisms involved. However, preliminary results are encouraging and the prospects very promising.

Acknowledgements

The authors would like to thank the staff of the Ioffe Physico-Technical Institute, St. Petersburg, Russia, D. Bimberg and F. Heinrichsdorff of the Technical University of Berlin, and A. Onishchenko and E. O'Reilly of the University of Surrey, UK, for useful discussions.

References

[1] Y. Arakawa, H. Sakaki, Appl. Phys. Lett. 40 (11) (1982) 939–941.
[2] M. Asada, Y. Miyamoto, Y. Suematsu, IEEE J. Quantum Electron. 22 (9) (1986) 1915–1921.
[3] D. Bimberg, N. Kirstaedter, N.N. Ledenstov, Zh.I. Alferov, P.S. Kop'ev, V.M. Ustinov, IEEE J. Selected Topics Quant. Electron. 3 (1997) 196–205.
[4] L. Goldstein, F. Glas, J.Y. Marzin, M.N. Charasse, G. Leroux, Appl. Phys. Lett. 47 (10) (1985) 1099–1101.
[5] D. Leonard, M. Krishnamurthy, C.M. Reaves, S.P. Denbaars, P.M. Petroff, Appl. Phys. Lett. 63 (23) (1993) 3203–3205.
[6] N. Kirstaedter, N.N. Ledentsov, M. Grundmann, D. Bimberg, V.M. Ustinov, S.S. Ruvimov, M.V. Maximov. P.S. Kop'ev, Zh.I. Alferov, U. Richter, P. Werner, U. Gösele, J. Heydenreich, Electron. Lett. 30 (17) (1994) 1416–1417.
[7] D. Klotzkin, K. Kamath, P. Bhattacharya, IEEE Photon. Technol. Lett. 9 (10) (1997) 1301–1303.
[8] H. Benisty, C.M. Sotomayor-Torres, C. Weisbuch, Phys. Rev. B 44 (19) (1991) 10945–10948.
[9] Q. Xie, A. Madhukar, P. Chen, N.P. Kobayashi, Phys. Rev. Lett. 75 (13) (1995) 2542–2545.
[10] O.G. Schmidt, N. Kirstaedter, N.N. Ledentsov, M.H. Mao, D. Bimberg, V.M. Ustinov, A.E. Egorov, A.E. Zhukov, M.V. Maximov, P.S. Kop'ev, Zh.I. Alferov, Electron. Lett. 32 (14) (1996) 1302–1304.
[11] P. Bhattacharya, K. Kamath, J. Singh, D. Klotzkin, J. Phillips, H.-T. Jiang, N. Cheverla, T. Norris, T. Sosnowski, IEEE Trans. Electron. Dev. 46 (1999) 871–883.
[12] H. Jiang, J. Singh, IEEE J. Quant. Electron. 34 (1998) 1188–1196.
[13] D. Bhattacharyya, E.A. Avrutin, A.C. Bryce, J.M. Gray, J.H. Marsh, D. Bimberg, F. Heinrichsdorff, V.M. Ustinov, S.V. Zaitsev, N.N. Ledentsov, P.S. Kop'ev, Zh.I. Alferov, A.I. Onishchenko, E.P. O'Reilly, J. Selected Topics Quantum Electron. 5 (1999) 648–657.
[14] N.Yu. Gordeev, A.M. Georgievski, V.I. Kopchatov, S.V. Zaitzev, A.Yu. Egorov, A.R. Kovsh, V.M. Ustinov, A.E. Zhukov, P.S. Kop'ev, Modal composition of radiation in room-temperature quantum dot lasers, Proceedings of the Fifth International Symposium on Nanostructures: Physics and Technology, St. Petersburg, Russia, 1997, pp. 183–186.
[15] L. Harris, D.J. Mowbray, M.S. Skolnick, M. Hopkinson, G. Hill, Appl. Phys. Lett. 73 (7) (1998) 969–971.
[16] W. Zhou, O. Qasaimeh, J. Philips, S. Krishna, P. Bhattacharya, Appl. Phys. Lett. 74 (6) (1999) 783–785.
[17] E.V. Arzhanov, A.P. Bogatov. V.P. Konyaev, O.M. Nikitina, V.I. Shveikin, Quantum Electron. 24 (7) (1994) 581–587.
[18] E.P. O'Reilly, A.I. Onishchenko, E.A. Avrutin, D. Bhattacharyya, J.H. Marsh, Electron. Lett. 34 (21) (1998) 2035–2037.
[19] G.P. Agrawal, IEEE J. Quantum Electron. 23 (6) (1987) 860–868.
[20] H.E. Lassen, H. Olesen, B. Tromborg, IEEE Photon. Technol. Lett. 1 (9) (1989) 261–263.
[21] L.V. Asryan, R.A. Suris, Appl. Phys. Lett. 74 (9) (1999) 1215–1217.
[22] P. Borri, W. Langbein, J.M. Hvam, Technical Univ. Denmark, Denmark.
[23] M.-H. Mao, F. Heinrichsdorff, D. Bimberg, Ultrafast dynamics in InAs/GaAs quantum dot amplifiers, Conference on Lasers and Electro-Optics (CLEO '99), Baltimore, 24-29 May 1999, paper CWL5.

[24] A.O. Kosogov, P. Werner, U. Gösele, N.N. Ledentsov, D. Bimberg, V.M. Ustinov, A.Yu. Egorov, A.E. Zhukov, P.S. Kop'ev, N.A. Bert, Appl. Phys. Lett. 69 (1996) 3072–3074.
[25] S. Malik, C. Roberts, R. Murray, M. Pate, Appl. Phys. Lett. 71 (1997) 1987–1989.
[26] A.C. Bryce, F. Camacho, P. Cusumano, J.H. Marsh, IEEE J. Selected Topics Quant. Electron. 3 (1997) 885–892.
[27] O. Kowalski, C.J. Hamilton, S.D. McDougall, J.H. Marsh, A.C. Bryce, R.M. De La Rue, B. Vögele, C.R. Stanley, Appl. Phys. Lett. 72 (1998) 581–583.